RSC Advances

ROYAL SOCIETY OF CHEMISTRY

www.rsc.org/advances

Cite this: DOI: 10.1039/c0xx00000x

www.rsc.org/xxxxxx

ARTICLE TYPE

Cationic surfactant assisted synthesis of poly o-methoxy aniline (PoMA) hollow sphere and its self healing performance

T.Siva[a], S.Sathiyanarayanan[a]*

Received (in XXX, XXX) XthXXXXXXXXX 20XX, Accepted Xth XXXXXXXXX 20XX

DOI: 10.1039/b000000x

Hollow microspheres of poly (o-methoxy aniline) (PoMA) were prepared in a solution of cetyltrimethyl ammonium bromide (CTAB) using ammonium persulfate (APS) as oxidant. The morphology of the final polymers was characterized by scanning electron and transmission electron microscopic techniques. The microsphere is formed by the polymer growth on preformed micelles. The presence of CTAB led to microspheres with a very regular size distribution. The polymer hollow sphere thus synthesized was characterized by FTIR, UV-Vis, TGA and XPS techniques. A study has been made on the corrosion protection performance of mild steel by epoxy coating containing synthesized PoMA hollow spheres using EIS measurements in 3% NaCl solutions. The self healing ability of the coating was studied by scanning vibrating electrode technique (SVET).

Introduction An intelligent functional coating for corrosion protection is rapidly drawing attention. Knowledge on various related fields such as drug delivery [1], biomimicing [2], advancement in polymer and nano material synthesis helped in designing newer strategies in this regard. Non-carcinogenic nature, non-interfering behaviour, timely and sustained release of corrosion inhibitor molecules at local corrosion sites raised greater expectations from these new generation functional coatings [3]. Among the various stimuli, pH and redox activity suits well for successful corrosion protection [4, 5]. The former is due to the local pH changes in the corrosion site which can be exploited while the later is due to the potential difference between the redox polymer and the base metal which galvanically passivates the base metal [6]. Additional advantage is the simultaneous release of inhibitors which are added to the polymer as dopants [7].

Design and fabrication of nanostructured materials especially redox active materials with functional properties became active area of research because of the fact that many of their properties are the function of their size, composition, and structural order. Hollow polymeric spheres, which have potential applications in reactors [8], pigments [9], catalysts [10], sensors [11], carriers [12], and photochemistry [13], and that of conducting polymer nanotubes, nanowires and nanospheres has been recently reported [14, 15].

In spite of various disadvantages, use of templates is an effective way to fabricate hollow microspheres because of better core size control [16-24]. The surface of the template was modified to make it active, which can later interact with shell substance like monomer or polymer chain. Several research groups have developed ways of improving the surface characteristics of templates, such as copolymerization with some other monomers to introduce active groups on the template surface [25], adding another special substance to adsorb polymer or monomers on the surface of templates [26-28], and directly modified the templates through some chemical reaction like sulfonation [29]. Utilizing the interaction between the modified surface of the templates and base substance, core–shell structured particles could be finally produced.

Herein we report the synthesis of poly o-methoxy aniline hollow spheres by a template assisted method based on a hydrothermal methodology. The influence of CTAB and o-methoxy aniline on the morphology of the resulting polymer was investigated. A possible formation mechanism is suggested based on the phenomena observed in this work. The active corrosion protection performance of PoMA hollow spheres incorporated organic coatings on mild steel was also reported.

Experimental

Synthetic procedure of Poly (o-methoxy aniline) (PoMA) hollow sphere

The cationic surfactant (CTAB, 0.874 g) was dissolved in distilled water (50 mL). 2.594 g of o-methoxy aniline was dissolved in 12 mL of (0.5 M) HCl which was added drop wise to the surfactant solution with constant stirring to form micelle solution. For the polymerisation reaction to produce PoMA hollow spheres, 0.194 g of ammonium persulphate (APS) initiator was added drop wise to the micelle solution within a period of 2 hours. This solution was transferred to an autoclave and maintained at 120 °C for 6 hours. Finally the product was precipitated in excess amount of ethanol to remove residual surfactants and initiators. Thus prepared PoMA hollow spheres were characterised and used as a pigment in paint formulation.

Characterization of PoMA hollow sphere

The FTIR spectrum of poly (o-methoxy aniline) hollow sphere was recorded using Nicolet 380 FTIR instrument having ATR attachment (Thermo,USA).

The X-ray diffraction pattern of the poly (o-methoxy aniline) hollow sphere was taken with PAN Analytical (Model PW 3040/60) X-ray diffractometer using Cu K_α radiation in the 2θ range of 0-90° at the scan rate of 0.017°/ 2θ.

The poly (o-methoxy aniline) hollow spheres were dissolved in N-methyl pyrrolidone (NMP) solution and the electronic absorption spectrum was recorded by Ultra violet-visible-near infrared (UV–Vis NIR) double beam spectrophotometer (Evolution 600, Thermo Scientific Ltd.)

The Thermal gravimetric analysis of poly (o-methoxy aniline) hollow sphere has been done using the Thermal Analyzer STA, 1500 (Polymer laboratory, Thermal Science Ltd).

X-ray Photoelectron Spectra (XPS) of the samples were recorded on MultiLab 2000 (Thermofisher Scientific, UK) fitted with a twin anode x-ray source using Mg K_α radiation (1253.6 eV). The sample pellets were mounted on the SS sample holder (stub) using conducting silver paint (Agar Scientific Ltd, UK). The stub was initially kept in the preparatory chamber overnight for desorbing any volatile species at 10^{-9} mbar and was then introduced into the analysis chamber having a base pressure of $9.8x10^{-10}$ mbar for recording the spectra. High-Resolution spectra averaged over 5 scans with a dwell time of 100 ms in steps of 0.05 eV were obtained at pass energy of 20 eV in Constant Analyzer Energy Mode. The binding energy was referenced with C (1s) at 284.98 eV within accuracy of ±0.05 eV.

The morphology of PoMA hollow spheres was analyzed using scanning electron microscope (Hitachi, model S3000H) and Transmission electron microscopy (Tecnai - 20 (G2).

Evaluation of corrosion protection and self healing property

A glass tube of 1.2 cm diameter was fixed on the coated mild steel with an adhesive (m-seal). 3% NaCl solution was poured into the glass tube as test medium. A platinum foil and a saturated calomel electrode (SCE) were placed inside the glass tube. This assembly constitutes the conventional three electrode cell and was connected to Electrochemical Impedance Analyzer (PAR 2273). Impedance measurements were carried out over the frequency range 100 KHz to 0.1 Hz with AC signal of rms amplitude of 20 mV using Powersuite software. The impedance values are reproducible to ±3 to 5%. From the impedance plots, the coating resistance (R_c) and the coating capacitance (C_c) values were estimated through ZsimpWin 3.21 software using the equivalent circuit for impedance data with one time constant as shown in Fig.1 where R_s is the solution resistance, R_c is the coating resistance and Q is the constant phase element representing the coating capacitance [30]. When there exists two time constants, the impedance data were analysed using the equivalent circuit (Fig.1) where C_{dl} is the double layer capacitance and R_{ct} is the charge transfer resistance.

The Scanning vibrating electrode technique (SVET) instrumentation used in these experiments was from Princeton Applied Research (SCV 370 control unit). Samples prepared for SVET measurement were of 1x1 cm squares with scan area of 4000 × 4000 µm and 64 x 48 points X and Y axis. The coated sample was scribed to introduce an artificial defect of size ranging from 0.1 to 0.3 mm^2. The sample was mounted in a teflon holder and the 3% NaCl solution was added. Scans were initiated within 5 min of immersion and the data were collected for various durations. Each scan consists of 400 data points on a 20 x 20 grid, with an integration time 1s per point. A complete scan required 10 min, followed by a 5 min rest period prior to the next scan. The current density maps were plotted in 3D format over the scan area, with positive and negative current densities representing anodic and cathodic regions, respectively. The measurements were taken at the open-circuit potential.

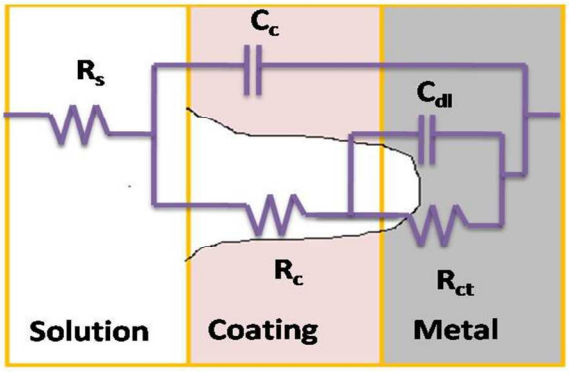

Fig. 1 Equivalent circuit for painted panels.

Results and Discussion

The PoMA hollow sphere has been synthesized by chemical oxidative polymerization using cationic surfactant in an aqueous medium. A schematic diagram of the synthetic procedure is presented in Fig. 2. When the CTAB concentration was above the critical micelle concentration (CMC, 0.0156 M for CTAB) in distilled water, spherical micelles were formed. oMA droplets (formed due to the low solubility of o-methoxy aniline in aqueous solutions) and micelles composed of o-methoxy aniline and CTAB serve as templates for the formation of the PoMA hollow spheres. When the hydrophilic APS oxidant was added drop wise, polymerization would take place on the surface of the oMA droplets and/or at the micelle / water interface. As polymerization proceeds with time, the polymerized PoMA would become larger hollow sphere by accretion and fusion. Holes would readily form in the hollow PoMA sphere as oMA monomer diffuses to the micelle/water interface and water/water soluble compounds enter the interior of the expanding microspheres. The resultant product was thoroughly washed with an excess of ethanol in order to remove the excess CTAB and other residual reagents [31-33].

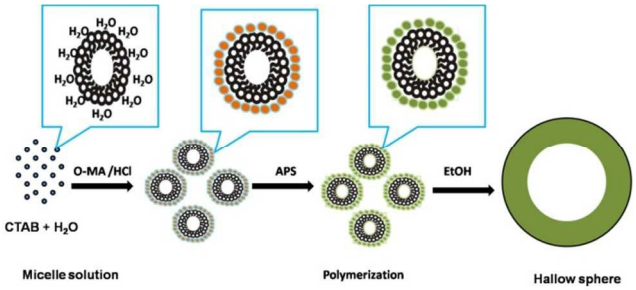

Fig. 2 Formation mechanism of PoMA hollow sphere.

The surface morphology of hollow PoMA analyzed by scanning electron microscope (SEM) is shown in Fig. 3a, b reveal hollow spherical morphology of the synthesized PoMA. These spheres are uniformly distributed, with the average diameter around 150 nm. PoMA spheres clearly indicate the hollow nature. The TEM micrograph (Fig 3c-f) also confirms that the PoMA sphere has a hollow core structure. The size of the hollow sphere measured from the TEM micrograph range from 50 to 150 nm [34].

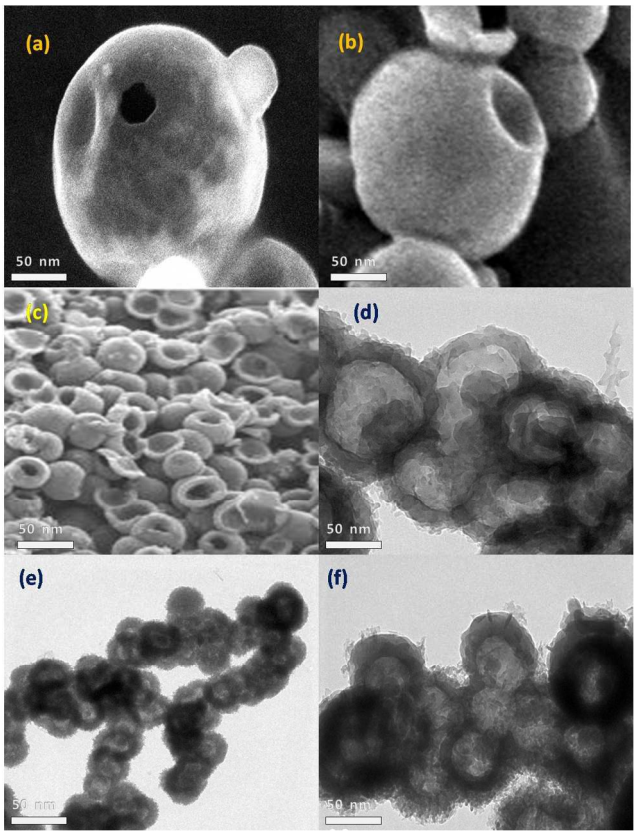

Fig. 3 SEM and TEM images of PoMA hollow sphere Caption (a)-(f) indicates different magnification of PoMA hollow sphere.

The FTIR data (Figure S1) of PoMA hollow spheres. The bands at 2930 and 2830 cm^{-1} are due to the C–H stretching vibration in the $–OCH_3$ group. The bands centred at 1491 and 1598 cm^{-1} correspond to C=C stretching vibrations of the benzenoid (B) and quinoid rings (Q), respectively. The medium absorption band appearing at 520 cm^{-1} could be attributed to bending deformation of N-H group attached to benzene ring. The bands at 1283 and 1035 cm^{-1} are assigned to the C–O–C stretching of an alkyl aryl ether linkage, and the strong bands near 947 and 880 cm^{-1} indicate the out-of-plane deformation of C–H in the o-substituted benzene ring [35]. The strong absorption band appearing at 759 cm^{-1} corresponds to rocking deformation of methylene group in case of polymer. In addition, a broad band at about 3426 cm^{-1} is attributed to N–H stretching vibrations [36]. These IR adsorptions confirm the formation of PoMA hollow spheres with a molecular structure as shown in fig. 4.

As like most of the polymers the PoMA is generally amorphous in nature (Figure. S2). Presence of two broad peaks conferred at $2\theta = 20^{o}$ and 25^{o} may be due to periodicity parallel and perpendicular to the polymer chain and also presence of the CH_3O- groups attached to the polymer backbone [37].

The UV–Vis spectrum of PoMA dissolved in N-methyl pyrrolidone (NMP) solution (Figure. S3) has three characteristic absorption peaks at 290 nm, 420 and 540 nm respectively. The peak at 290 nm is due to the π-π* transition in the benzenoid ring and at 420 nm is due to the π–polaron bond transition. The broad absorption band appears in the visible region at 540 nm may be due to the high conjugation of the aromatic polymeric chain as reported earlier [38, 39].

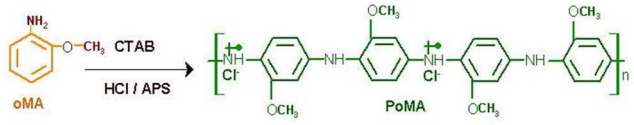

Fig. 4 Molecular structure of PoMA.

Fig. 5a shows the XPS survey spectrum confirming the presence of C1s, N1s and O1s at the corresponding binding energies 284.18, 398.96 and 532.2 eV respectively. The C1s peak can be fitted well with three components (Fig. 5b). The peaks observed at 284.6 eV correspond to aromatic carbon. The second peak centred on 287.1 eV can be assigned to aromatic carbons bound to amine nitrogen, while the third peak around 287.0 and 288.6 eV can be assigned to C-N formation [40-42]. The N1s spectrum shows (Fig. 5c) a broad peak contributed by two components at 399.7, and 401.0 eV. The first and second BE peaks can be ascribed to neutral imine (=N–) and amine (–NH–) nitrogen atoms, respectively [43]. The O1s spectra also consist of three peaks (Fig. 5d) corresponding to hydroxide (OH-) (531.8), and adsorbed H_2O (532.8eV) [44].

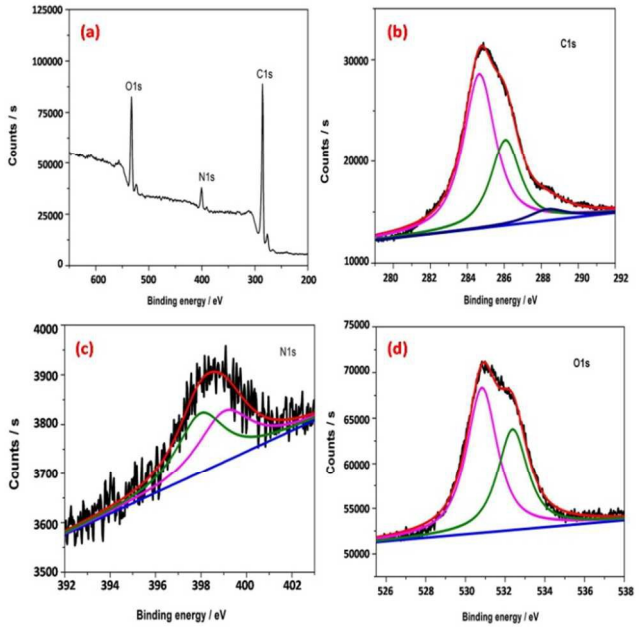

Fig. 5 XPS spectra of PoMA hollow sphere.

(a) Survey; (b) C1s; (c) N1s; (d) O1s core level spectra.

Formulation of paint containing PoMA hollow sphere

The epoxy resin (6071; Ciba Geigy) solution was prepared by dissolving solid epoxy having epoxy equivalent weight 450–500

in xylene. The PoMA pigment (15% V/V) was completely dispersed in the resin by using attritor. The PoMA pigmented epoxy resin solution was cured with polyamide (Sympol 115) having amine value 210–230 mg. The paint was prepared in such a way that it had 30% volume solids. The PoMA pigmented paint was applied by brush on mild steel panels. Before application, the steel specimens (150 mm × 100 mm) were acid cleaned. The coatings were evaluated by EIS and OCP measurements after 10 days of curing at room temperature. The thickness of the coating was measured using a coating thickness meter (Elcometer 456) and it was found to be 40±2 µm.

Evaluation of corrosion protection ability of the coating by EIS method

Figs 6 (a,b) depicts the Bode representation of electrochemical impedance behaviour of epoxy coating without and with the addition of PoMA hollow sphere on mild steel in 3% NaCl. Existence of single or double slopes in the mid frequency range would suggest the pure barrier behaviour (single time constant) or corrosion initiated through pores in barrier (two time constant) behaviour of coating. From these impedance plots the kinetic parameters such as the coating resistance (R_c) and the coating capacitance (C_c) values were estimated by iterative fitting of data through ZsimpWin 3.21 software using the equivalent circuit for impedance data with one time constant as shown in Fig.1 where R_s is the solution resistance, R_c is the coating resistance and Q is the constant phase element representing the coating capacitance [31]. When there exists two time constants, the impedance data were analysed using the equivalent circuit (Fig 1) where C_{dl} is the double layer capacitance and R_{ct} is the charge transfer resistance. The resistance and capacitance values of the coating with continued exposure time derived from these graphs by fitting appropriate equivalent circuits (Fig 1) are given in Table 1. In the case of blank epoxy coating (without PoMA), the initial value of the coating resistance value is 1.69×10^7 Ω cm^2 and with prolonged exposure to 3% NaCl solution, the coating resistance value decreases and reached 7.39×10^4 Ω cm^2 after 30 days immersion. The intact nature of the coating at the initial instant resulted in high resistance while the continuous exposure causes the entrapment of moisture through the film resulting in the decreased resistance of the coating. Besides, after 5 days immersion, the impedance behaviour shows the existence of two time constants confirming the occurrence of charge transfer reaction due to iron dissolution through pores in the coating. The charge transfer resistance (R_{ct}) value for the coating without PoMA is found to be 1.54×10^5 Ω cm^2 which decreased to 3.77×10 Ω cm^2 after 30 days exposure in 3% NaCl. This decrease in charge transfer resistance confirms the increased corrosion activity with time of exposure. In the case of PoMA containing epoxy coating, the impedance values remained at 10^6 Ω cm^2 even after 30 days exposure to 3% NaCl which is two order higher than that of PoMA free epoxy coating. Maintenance of coating resistance in the threshold range (10^6Ω cm^2) shows the superior performance of PoMA containing epoxy coating. Besides, the capacitance value of PoMA containing epoxy coating is very low (2.59×10^{-10} F cm^{-2}) than that of epoxy coating without PoMA.

Table 1 EIS analysis of epoxy and PoMA hollow sphere coating on mild steel in 3% NaCl.

Duration (Days)	EIS-Epoxy coating				EIS- PoMA hollow sphere coating	
	R_c Ω cm^2	C_c F/cm^{-2}	R_{ct} Ω cm^2	C_{dl} F/cm^{-2}	R_c Ω cm^2	C_c F/cm^{-2}
Initial	1.69×10^7	7.63×10^{-10}	–	–	1.77×10^7	8.38×10^{-11}
1 day	2.95×10^6	6.47×10^{-9}	–	–	4.59×10^6	1.37×10^{-10}
3 day	1.76×10^5	8.74×10^{-9}	–	–	1.91×10^6	1.69×10^{-10}
5 day	1.54×10^5	1.45×10^{-8}	1.54×10^5	8.94×10^{-10}	1.09×10^6	2.59×10^{-10}
10 day	1.02×10^5	2.05×10^{-8}	1.18×10^5	9.10×10^{-10}	2.87×10^6	3.54×10^{-10}
15 day	7.60×10^4	4.88×10^{-8}	6.19×10^4	5.60×10^{-10}	2.51×10^6	4.60×10^{-10}
30 day	7.39×10^4	7.02×10^{-8}	3.77×10^4	4.31×10^{-9}	2.40×10^6	2.59×10^{-10}

The better corrosion protection offered by PoMA containing coating can be visualized in the Fig 6b. As the PoMA incorporated epoxy coated mild steel is immersed in 3% NaCl solution, the polymer and the base metal junction creates a galvanic coupling [45]. When there is a pinhole or mechanical damage in the coating which permits the inflow of electrolyte i.e 3% NaCl solution, the potential difference between the metal/electrolyte interface and PoMA / electrolyte interface triggers the reduction of PoMA spontaneously and oxidation of metal occurs resulting in the passivation of metal [46, 47].

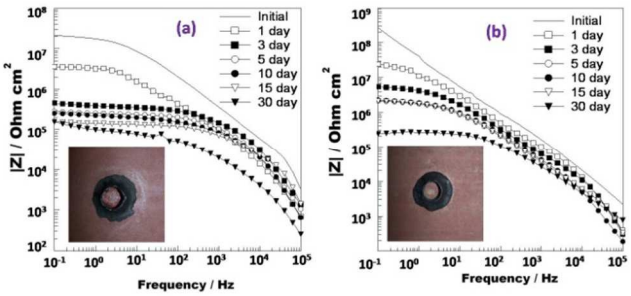

Fig. 6 (a, b) EIS plot of without/with PoMA hollow sphere coating.

(a) Pure epoxy coating; (b) With PoMA epoxy coating.

This formation of passive layer on the metal surface at the pinhole / mechanical damage exposed area protects the mild steel from further corrosion [48]. The PoMA regains its original oxidized state by re-oxidation by the atmospheric or dissolved oxygen. This activity restores the self healing activity of PoMA once again [49].

The open circuit potential (OCP) monitoring is a useful parameter to confirm the active or passive state of a corroding interface. The OCP of blank epoxy has an initial value of -0.313 V vs SCE and with continued exposure to 3% NaCl gradually gets shifted in the active direction indicating the degradation in the corrosion protective property of the epoxy coating or increasing corrosion activity. The impedance results also reflect this behavior wherein the coating resistance values steadily decrease from its initial value.

On the other hand, the PoMA hollow sphere incorporated

epoxy coating showed a noble shift in the OCP value (Fig.7) which was initially at -0.280 V vs SCE to -0.044 V vs SCE in 3 days and gradually stabilizes at around -0.090 V. The reason for this noble shift may be due to the initiation of corrosion just after the initial measurement which triggered the redox transition of PoMA from its oxidized state to reduced state resulting in passivation of base metal as described above. This observation confirms the self healing characteristics of PoMA hollow sphere containing epoxy coating. Similar shifts of open circuit potentials in noble direction for conducting polymer based coatings were already reported [50-53]. After the evaluation period, i.e. 30 days, the glass tubes fixed to the painted panel were removed and visual observations were made. It was found that there was no blister formation or delamination of coating (shown as inset in EIS graphs) in the case of PoMA hollow sphere containing coating while PoMA free epoxy coating exhibits failure of the coatings.

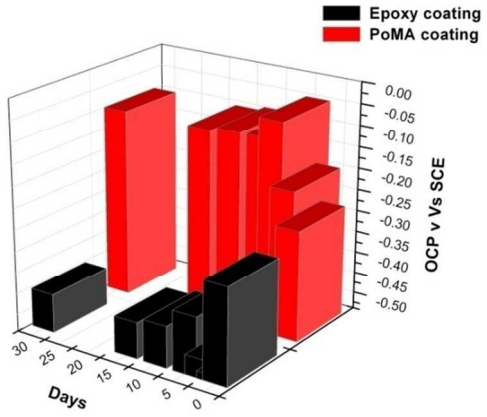

Fig. 7 OCP variation of coated mild steel panels in 3% NaCl.

Evaluation of self healing ability of the coating by SVET method

The SVET results of pure epoxy coating (PoMA free) on steel surface in 3% NaCl for various durations of exposure are given in Fig.8 a, b. The Fig.8a depicts the local current maps over the surface of epoxy coated mild steel recorded immediately after exposure to 3% NaCl (i.e. after 5 min). A steep anodic current flow in the artificial flaw area indicates the occurrence of accelerated metal corrosion due to the small anode large cathode configuration of the defect area. With continuous exposure to aggressive 3% NaCl solution, the width of corrosion activity increases (Fig not shown) (width of current flow) and occurrence of such current flows were identified over the entire scanned area confirming the initiation and procession of corrosion activity throughout the coated area. This result indicates the absence of any specific self healing activity in the pure epoxy resin coating on mild steel surface. Fig. 9a and b shows the similar current density maps for 3% PoMA containing epoxy coated steel in 3% NaCl. Presence of steep and narrow current flow at the artificial defect area immediately after initial immersion (Fig. 9a) in 3% NaCl shows the corrosion activity at the defect area where the bare metal reacts with aggressive electrolyte and corrode. The width of the corrosion activity decreases with time (figure not shown) and after 24 hours of immersion, (Fig. 9b) which was completely suppressed. This confirms the passivation of exposed metal (self healing property of PoMA) surface at the defect area

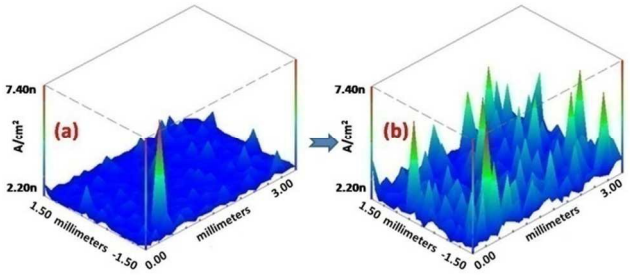

Fig. 8 Current distribution map for epoxy coating in 3% NaCl at various immersion periods.

(a) Initial; (b) 24h

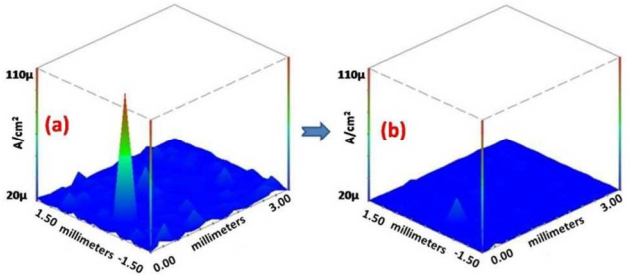

Fig. 9 Current distribution map for PoMA containing epoxy coating in 3% NaCl at various immersion periods.

(a) Initial; (b) 24h

by the PoMA molecules present adjacent to the mouth of the defect as per the model suggested. Based on these observations, a suitable mechanism has been proposed as presented in Fig.10 which is self-explanatory.

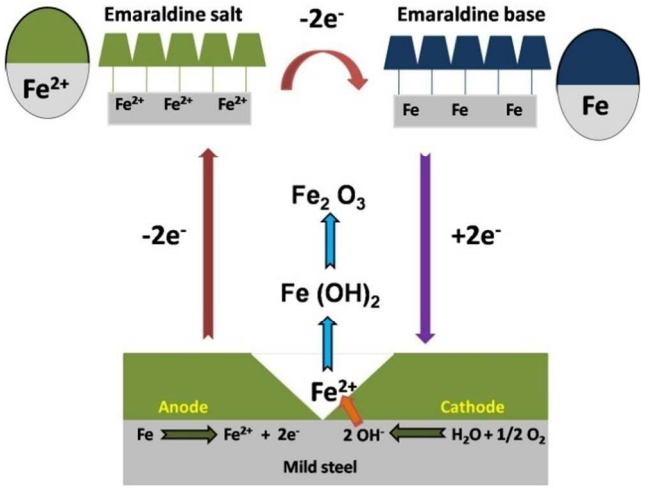

Fig. 10 Mechanism of self healing coating.

In conclusion, for the Hollow spherical poly (o-methoxy aniline) has been synthesized by chemical oxidative polymerization through a hydrothermal method. This unique polymerization route is very effective in synthesizing size controlled hollow poly (o-methoxy aniline) spheres. The UV-Vis spectrum, SEM and TEM studies show the emeraldine salt form has hollow sphere structure of PoMA. The XRD pattern confirms amorphous nature of PoMA. The FT-IR results confirm the expected structure of the

polymer and formation of hollow PoMA solid. The thermal stability of the polymer is confirmed by thermo gravimetric analysis. The PoMA hollow sphere incorporated epoxy coating was found to offer better corrosion protection and possess self healing property than that of PoMA free epoxy coating.

Acknowledgements

The authors wish to express their sincere thanks to the Director, CECRI, Karaikudi for his encouragement. The authors thank CSIR, New Delhi for financial support through the 12th Five Year Plan network project IntelCOAT (CSC0114).

Notes and references

[a]*Corrosion and materials protection division, CSIR-Central Electrochemical Research Institute, Karaikudi-630006, India. sathya_cecri@yahoo.co.in*

† Electronic Supplementary Information (ESI) available: [FTIR,XRD,UV-Vis, TGA data of PoMA Hollow sphere]. See DOI: 10.1039/b000000x/

[1] H.Q. Wang, X. Yan, G.L. Li, C. Pilz-Allen, H. Mohwald, D.G. Shchukin, *Adv. Health care Mat.,* 2014, **3**, 825.
[2] Z. Zheng, X. Huang, M. Schenderlein, H. Moehwald, G.K. Xu, D.G. Shchukin, *Nanosc.,* 2015, **7**, 2409.
[3] T.Siva, M. Sunder, S.S. Sreejakumari, S. Sathiyanarayanan, *RSC Adv.,* 2015, **5**, 39278.
[4] Z. Zheng, M. Schenderlein, X. Huang, N.J. Brownbill, F. Blanc, D.G. Shchukin, *ACS Appl. Mater. Inter.,* 2015, **7**, 22756.
[5] D. Grigoriev, D. Akcakayiram, M. Schenderlein, D.G. Shchukin, *Corr.,* 2014, **70**, 446
[6] A. Yabuki, K. Okumura, *Corrosion Sci.,* 2012, **59**, 258.
[7] K. Aramaki, *Corrosion Sci.,* 2002, **44**, 1621.
[8] F. Caruso, R.A. Caruso, H. Mohwald*, Sci.,* 1998, **282**, 1111.
[9] F. Caruso, *Adv. Mater.,* 2001, **13**, 11.
[10] R. Davies, G.A. Schurr, P. Meenan, R.D. Nelson, H.E. Bergna, C.A.S. Brevett, R.H. Goldbaum, *Adv. Mater.,* 1998, 10, 1264.
[11] L.M. Liz-Marzan, M. Giersig, P. Mulvaney, *Lang.,* 1996 12, 4329.
[12] D.A. Antelmi, O. Spalla, *Lang.,* 1999, **15**, 7478.
[13] E. Bartsch, V. Frenz, J. Baschnagel,W. Schaertl, H. Silescu*, J. Chem. Phys.,* 1997, **106**, 3743.
[14] L. Zhang, H. Peng, C. F. Hsu, P. A. Kilmartin, T. Sejdic, *Nanotech.,* 2007, **18**, 115607.
[15] M. Trchova, I. Sedenkova E.N. Konyushenko, J. Stejskal, P. Holler, G.C. Marjanovic, *J. Phys. Chem. B.,* 2006, **110**, 9461.
[16 D. G. Shchukin, G. B. Sukhorukov, *Adv. Mater.,* 2004, **16**, 671.
[17] C. S. Peyratout, L. Dahne, *Angew. Chem. Int. Ed.,* 2004, **43**, 3762.
[18] W. Meier, *Chem. Soc. Rev.,* 2000, **29**, 295.
[19] F. Caruso, *J. Chem. Eur.,* 2000, **6**, 413.
[20] E. Donath, S. Moya, B. Neu, G.B. Sukhorukov, R. Georgieva, A. Voigt, H. Baumler, H. Kiesewetter, H. Mohwald, *J. Chem. Eur.,* 2002, **8**, 5481.
[21] M.R Karim, K.T Lim, C.J Lee M.S, Lee, *Synth. Met.,* 2007, **157**, 1008.
[22] E.N. Konyushenko, J. Stejskal, I. Sedenkova, M. Trchova, I. Sapurina, M. Cieslar, J. Prokes, *Polym. Int.,* 2006, **55**, 31.
[23] K. Huang, M. Wan, *Synth. Met.,* 2003, **173**, 135.
[24] N.I. Kovtyukhova, A. D. Gorchinskiy, C. Waraksa, *Mater. Sci. Eng.,* 2000, **B 424**, 69.
[25] W. Wu, D. Caruntu, A. Martin, *J. Magn. Magn. Mater.,* 2007, **311**, 578.
[26] C. Barthet, S.P. Armes, S.F. Lascelles, S.Y. Luk, H.M.E. Stanley, *Lang.,* 2007, **14**, 2032.
[27] S.F. Lascelles, S.P. Armes *J. Mater. Chem.,* 1997, **7**, 1339.
[28] S.F. Lascelles, S.P. Armes, P.A. Zhdan, S.J. Greaves, A.M. Brown, J.F. Watts, S.R. Leadley, S.Y. Luk, *J. Mater. Chem.,* 1997, **7**, 1349.
[29] L.Y. Wang, Y.H. Gu, Q.Z. Zhou, G.H. Ma, *Coll. Surf. B Biointer.,* 2006, **50**, 126.
[30] T. Siva, S. Sathiyanarayanan, *Prog. Org. Coat.,* 2015, **82**, 57.
[31] M. Liu, C. Luo, R. Huang, H. Peng, Y. Wang, J.T. Sejdic, *Inte. J. Polym. Mater. Polym. Biomater.,* 2014, **63**, 602.
[32] C. Luo, H. Peng, L. Zhang, G.L. Lu, Y. Wang, J.T. Sejdic, *Macromol.,* 2011, **44**, 6899.
[33] B.J. Han, G. Song, R. Guo, *Adv. Mater.,* 2006, **18**, 3140.
[34] L. Zhang, H. Peng, J. Sui, C. Soeller, P. A. Kilmartin, J.T. Sejdic, *J. Phys. Chem.,* 2009, **C 113**, 9128.
[35] Q. Cheng, V. Pavlinek, Y. He, Y. Yan, C. Li, P. Saha, *Smart Mater. Struct.,* 2011, 20, 065014.
[36] Y. Tan, F. Bai, D. Wang, Q. Peng, X. Wang, Y. Li, *Chem. Mater.,* 2007, **19**, 5773.
[37] X.Guo, G.T. Fei, H. Su, L.D. Zhang, *J. Mat. Chem.,* 2011, **21**, 8618.
[38] M. R. Nabid, Z. Zamiraei, R. Sedghi, *J. Ira. Polym.,* 2010, **19**, 699.
[39] M. Icli, A. Monal, A. Cihaner, *Polym Int.,* 2009, **58**, 674.
[40] A. Qaiser, M. Hyland, D.Patterson, *Synth. Met.,* 2012, **162**, 958.
[41] J. Li, X. Quian, L. Wang, X. An, *Bio Resour.,* 2010, **5**, 712.
[42] K. Tan, B.Tan, *J. Chem. Phys.,* 1991, **94**, 5382.
[43] S.J. Kerber, T.L. Barr, G.P. Mann, W.A. Brantley, E. Papazoglou, J.C. Mitchell, *J. Mat. Eng. Perf.,* 1998, **7**, 329.
[44] A.A. Hermas, Z.X. Wu, M. Nakayama, K. Ogura, *Electrochem. Soc.,* 2006, **153**, B199.
[45] J.C. Seegmiller, J.E. Pereira da Silva, D.A. Buttry, S.I. Cordoba de Torresi, R.M. Torresi, *Electrochem. Soc.,* 2005, **152**, B45.
[46] A. Hermas, M. Nakayama, K. Ogura, *Electrochim. Act.,* 2005, **50**, 2001.
[47] J.E.P. Da Silva, S.I.C. De Torresi, R.M. Torresi, *Corros. Sci.,* 2005, **47**, 811.
[48] P.J. Kinlen, D.C. Silverman, C.R. Jeffreys, *Synth. Met.,* 1997, **85**, 1327.
[49] P. Kern, A.L. Baner, J. Large, *Coat. Technol.,* 1999, **71**, 67.
[50] R. Mafi, S.M. Mirabedini, R. Naderi, M.M. Attar, *Corros. Sci.,* 2008, **50**, 3280.
[51] N. Ahmad, A.G. MacDiarmid, *Synth. Met.,* 1996, **78**, 103.
[52] Y. Wei, J. Wang, X. Jia, J.M. Yeh, *Polym.,* 1995, **36**, 4535.
[53] S. Souza, *Surf. Coat. Tech.,* 2007, **201**, 7574.